Synthesis of Allenes by Hydroalkylation of 1,3-Enynes with Ketones Enabled by Cooperative Catalysis

Maxwell Eaton, Yuping Dai, Ziyong Wang, Bo Li, Walid Lamine, Karinne Miqueu, Shih-Yuan Liu

Synthesis of Allenes by Hydroalkylation of 1,3-Enynes with Ketones Enabled by Cooperative Catalysis

Maxwell Eaton,[1] Yuping Dai,[2] Ziyong Wang,[1] Bo Li,[1] Walid Lamine,[2] Karinne Miqueu,*[2] Shih-Yuan Liu*[1,2]

[1] Department of Chemistry, Boston College, Chestnut Hill, Massachusetts 02467-3860, United States
[2] Université de Pau et des Pays de l'Adour, E2S UPPA / CNRS, Institut des Sciences Analytiques et de Physico-Chimie pour l'Environnement et les Matériaux IPREM UMR 5254. Hélioparc, 2 avenue P. Angot, 64053 Pau cedex 09, France

ABSTRACT: A method for the synthesis of allenes by the addition of ketones to 1,3-enynes by cooperative Pd(0)Senphos/$B(C_6F_5)_3$/NR_3 catalysis is described. A wide range of aryl and aliphatic ketones undergo addition to various 1,3-enynes in high yields at room temperature. Mechanistic investigations revealed a rate-determining outer-sphere proton transfer mechanism, which was corroborated by DFT calculations.

Introduction

Allenes are common structural motifs in natural products, bioactive small molecules, and materials.[1] They are also versatile synthetic intermediates, and many powerful transformations of allenes have been developed in recent years.[2-4] Therefore, methods for efficient allene synthesis have been sought after by researchers.[5] Of the many elegant catalytic methods, palladium-catalyzed hydrofunctionalization of conjugated enynes has emerged as an atom-economical approach for the preparation of allenes.[6] In particular, hydroalkylation of 1,3-enynes allows allene synthesis with concomitant C-C bond formation, and some enantioselective processes have recently been developed (Scheme 1a).[7] However, current methods require highly stabilized carbon pronucleophiles bearing multiple electron-withdrawing groups, or activated 1,3-enynes.

In general, intermolecular hydroalkylation of unsaturated hydrocarbons using relatively unactivated pronucleophiles, specifically ketones, is rare, with only a few reported examples.[8-10] Since Dong's seminal work describing rhodium-catalyzed hydroalkylation of unactivated olefins with ketones (Scheme 1b),[11] the hydroalkylation of dienes (Scheme 1c)[12] and alkynes (Scheme 1d)[13] with ketones have also been developed.[14,] However, due to the

lower reactivity of a ketone's α-C-H bond compared to more activated methylene compounds (e.g., malonates), [15] these methods typically require elevated temperatures. Additionally, there is no reported protocol for the hydroalkylation of 1,3-enynes with simple ketones. Given the synthetic utility of the ketone functionality and its prevalence in natural products and bioactive compounds,[16] a method allowing the mild, direct allenylation of ketones would represent a useful approach for building molecular complexity and late-stage functionalization of ketone-containing molecules. Here, we describe the development of a mild and general method for the hydroalkylation of 1,3-enynes with ketones via Pd(0)Senphos/$B(C_6F_5)_3$/amine base cooperative catalysis. The protocol is atom economical (no stoichiometric additives) and tolerates a wide range of both enynes and ketones to afford allenes in high yield after only a few hours at room temperature in most cases (Scheme 1e).

Scheme 1. Metal-Catalyzed Intermolecular Hydroalkylation

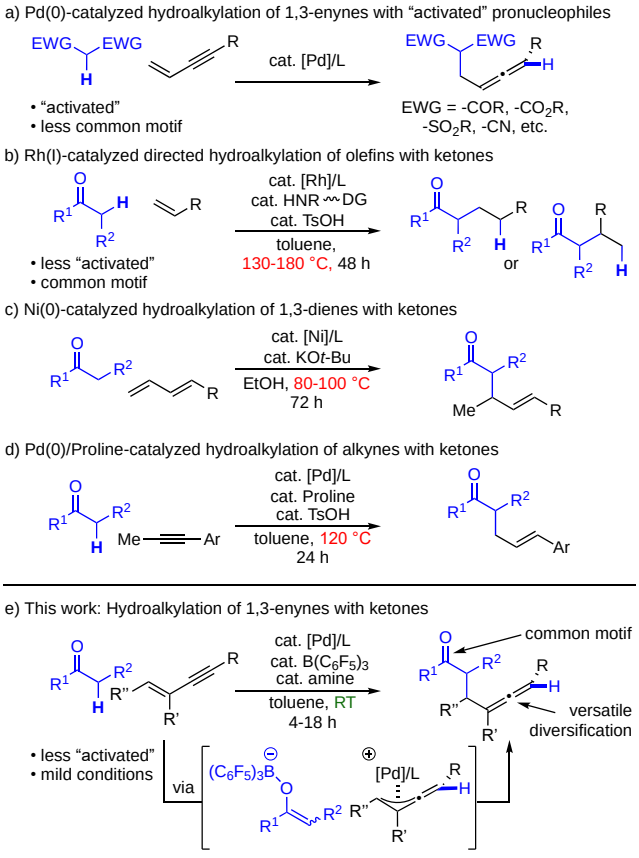

Results and Discussion

Recently our group has reported a series of borofunctionalizations of 1,3-enynes using palladium(0) supported by our Senphos ligands.[17] These reactions are hypothesized to proceed through an outer-sphere oxidative addition pathway involving activation of a palladium(0)-bound enyne by an electrophilic boron reagent.[18] We also recently developed a hydroalkynylation reaction utilizing cooperative Pd(0)Senphos/$B(C_6F_5)_3$/NR_3 catalysis.[19] We therefore envisioned that a dual catalytic system of palladium(0) and $B(C_6F_5)_3$/NR_3 could activate both the 1,3-enyne and the ketone simultaneously to promote addition of the ketone α-C-H across the enyne.[20]

Table 1. Survey of Ligands[a]

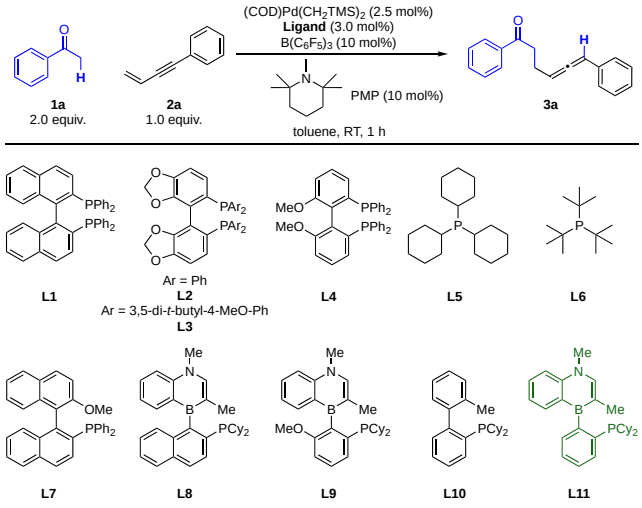

Entry	Ligand	Yield (%)[b]
1	**L1**	0
2	**L2**	0
3	**L3**	0
4	**L4**	0
5	**L5**	0
6	**L6**	<5
7	**L7**	<5
8	**L8**	47
9	**L9**	78
10	**L10**	48
11	**L11**	**92**

[a]See Supporting Information for detailed procedures. [b]Yields were determined by ^{1}H NMR analysis using 1,3,5-trimethoxybenzene as an internal standard.

To evaluate the feasibility of the proposed transformation, acetophenone **1a** and enyne **2a** were used as model substrates (Table 1). In the presence of 2.5 mol% (1,5-cyclooctadiene)bis(trimethylsilylmethyl)palladium(II), [(COD)Pd($CH_2TMS)_2$], 3.0 mol% **L11**, 10 mol% tris(pentafluorophenyl)borane [$B(C_6F_5)_3$], and 10 mol% 1,2,2,6,6-pentamethylpiperidine (PMP) in toluene, the desired allene product **3a** was formed in 92% yield after 1 hour at room temperature (entry 11). The use of bisphosphines (**L1**-**L4**) resulted in no observed product formation, and trialkyl phosphines (**L5**-**L6**) only gave either trace or no product. The commercially available monophosphine MOP (**L7**) also afforded trace product. Modifications to the Senphos ligand's lower aryl fragment (**L8**-**L9**) led to lower product yields. Use of the structurally related, commercially available MePhos (**L10**) resulted in only moderate yield of the product, underscoring the importance of the unique electronic structure conferred by the 1,4-azaborine ring.[21] No product formation was observed with any of the other Lewis acids tested, and other solvents examined resulted in diminished yields (see the Supporting Information, Table S1).

With the optimized conditions in hand, we next explored the substrate scope with respect to the ketone (Table 2). A wide range of substituted acetophenones (aryl ethers, amines, and halides) are tolerated under the reaction conditions (entries **3a**-**3g**). Larger naphthyl ketones (entry **3h**), secondary aryl ketones (entry **3i**), *ortho*- substituted aryl ketones (entry **3j**), and heteroaryl ketones (entries **3k**-**3m**) also react efficiently. Acyclic (entry **3n**) and cyclic aliphatic ketones (entries **3o**-**3q**) are also accepted. Notably, an enone (entry **3r**) also serves as a suitable substrate, albeit furnishing the product with diminished yield. The observed diastereomeric ratios (d.r.) with secondary ketone substrates are generally low. On the other hand, with unsymmetrical aliphatic ketones (entries **1s** and **1t**), the observed regiomeric ratio (r.r.) is moderate to excellent with the more substituted α-C-H undergoing addition to the enyne preferentially. This is likely due to preferential formation of the thermodynamically more stable enolate under the reaction conditions. More complex biologically active ketones (e.g., entry **1u**) also undergo efficient conversion to the corresponding allenes, demonstrating the potential of the method for late-stage functionalization.

Table 2. Reaction Scope of Ketones[a,b]

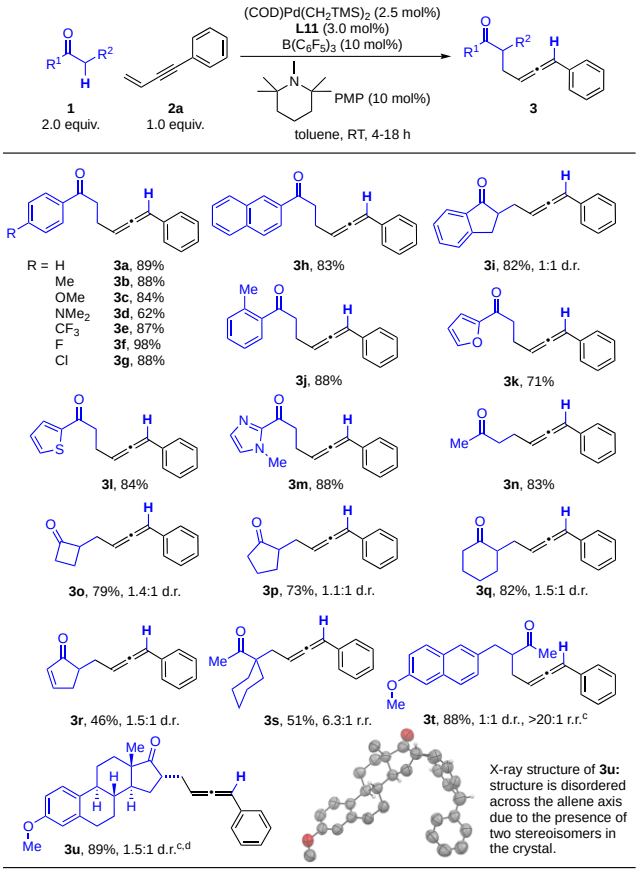

[a] Yields of isolated products are reported as an average of two trials. [b]See Supporting Information for details. [c]48 hr reaction time. [d] 6:1 CH_2Cl_2 : toluene used as solvent.

We next investigated the scope with respect to the 1,3-enyne. As can be seen from Table 3, a range of *para*- and *ortho*-substituted aryl enynes are well-tolerated (entries **4a**-**4d**). Alkyl enynes (e.g., entry **4f**) are also suitable substrates along with 1,3-disubstituted enynes (entries **4e** and **4g**). A 1,4-disubstituted enyne (entry **4h**) and a 1,2,4-trisubstituted enyne (entry **4i**) also furnish the corresponding coupling products although in only moderate yield. Various acid-sensitive functional groups such as silyl ethers, esters, protected amines, and alkyl halides are compatible with the reaction protocol (entries **4j**-**4m**).

Table 3. Reaction Scope of 1,3-Enynes[a,b]

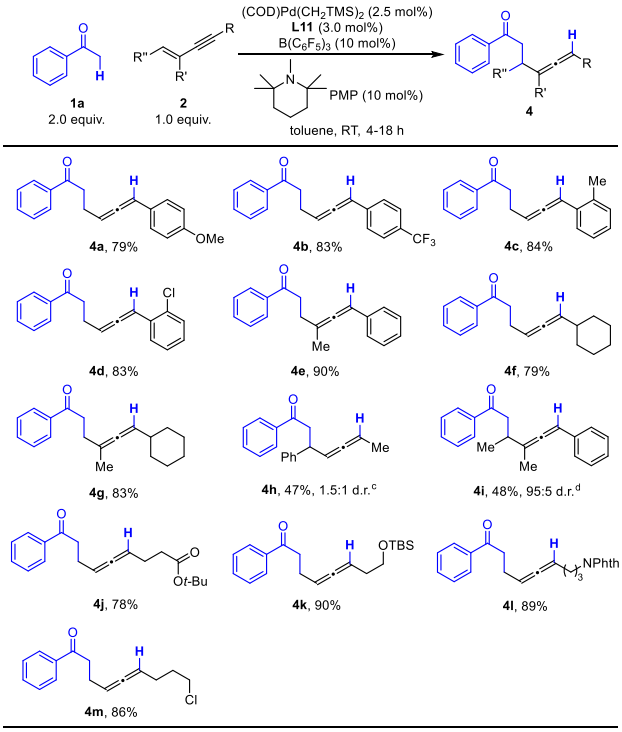

[a] Yields of isolated products are reported as an average of two trials. [b]See Supporting Information for details. [c]Reaction carried out at 45 °C for 18 hours. [d]Reaction carried out at 50 °C for 48 hours.

The process is also amenable to gram-scale procedure, with compound **3n** being produced on 7.5 mmol scale in 80% yield using 1.0 mol% of the palladium catalyst (Scheme 2). Compound **3n** serves as a useful intermediate for a variety of derivatizations. $TiCl_4$-mediated methylation[22] affords tertiary alcohol **5**, which can further undergo Au-catalyzed intramolecular hydroalkoxylation to yield furan derivative **6** in high yield and diastereoselectivity.[23] Cu-mediated intramolecular reductive coupling produces cyclohexenol **7** in good yield and excellent diastereoselectivity.[24] Cu-catalyzed borylation[25] affords cyclic trisubstituted alkenyl-Bpin **8**, which can then undergo Suzuki-Miyaura coupling to furnish densely functionalized cyclohexenol **9** in high yield.

Scheme 2. Gram-scale Synthesis and Product Derivatization

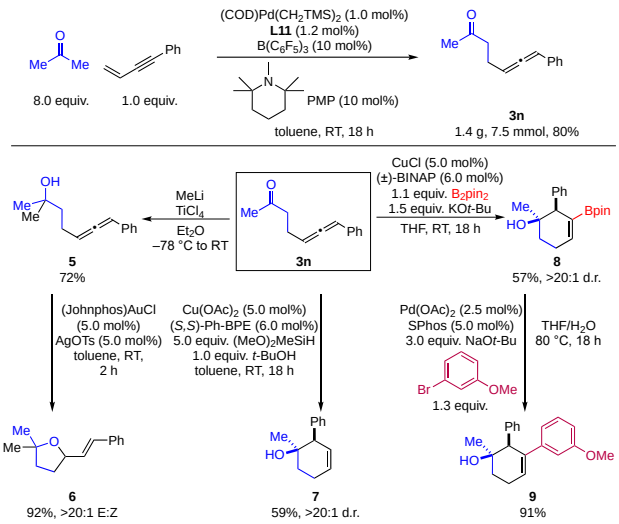

To elucidate the reaction mechanism, we carried out a series of mechanistic studies. First, we sought to identify the ^{31}P NMR signals of some likely catalytic intermediates. Free ligand **L11** exhibits a signal at –2.8 ppm (Scheme 3a). A 1:1 mixture of the palladium precursor (COD)Pd($CH_2TMS)_2$, **L11**, and excess enyne **2a** in toluene results in a broad resonance at 42.4 ppm, which we assign as the enyne-bound palladium complex **B** (Scheme 3b). Outer-sphere oxidative addition adduct **10** was independently isolated and fully characterized by NMR spectroscopy and X-ray crystallography (See Supporting Information for details) and features a sharp signal at 48.8 ppm (Scheme 3c). When the catalytic reaction under standard conditions was analyzed by ^{31}P NMR, only a single resonance at 48.6 ppm was observed (Scheme 3d), consistent with complex **10** being the resting state of the Pd catalyst.

Scheme 3. Pd Catalyst Resting State Determination by ^{31}P NMR

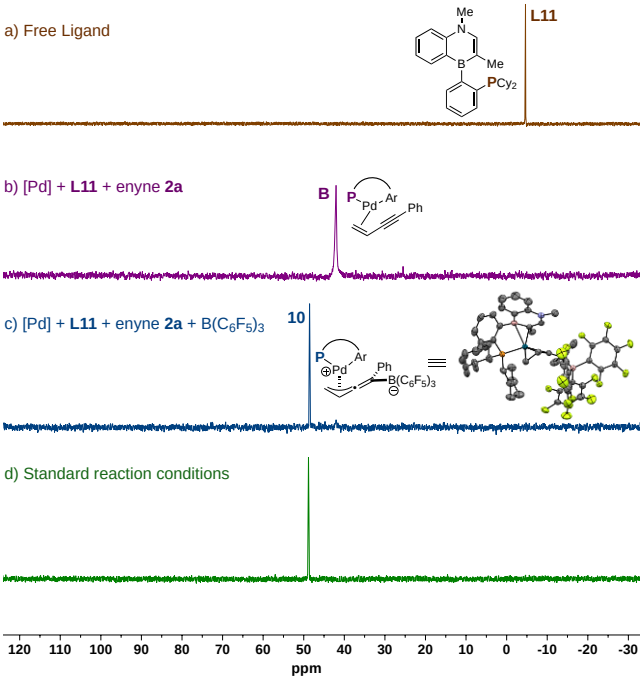

Scheme 4. B(C_6F_5)$_3$ Catalyst Resting State Determination by ^{11}B NMR

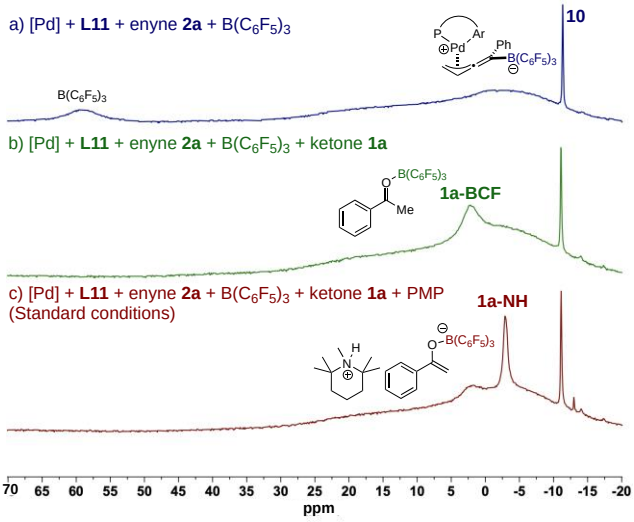

We next evaluated the resting state(s) of the boron catalyst by ^{11}B NMR. A combination of the palladium precursor, **L11**, B(C_6F_5)$_3$, and excess enyne produces a sharp resonance

at –11.0 ppm, originating from the tetracoordinate boron of complex **10** (Scheme 4a). The free $B(C_6F_5)_3$ appears as a broad signal at 60 ppm. Addition of excess ketone results in an additional broad signal at 2.3 ppm, consistent with the acetophenone-$B(C_6F_5)_3$ Lewis pair **1a-BCF** (Scheme 4b).[26] Upon addition of PMP base (simulating the standard reaction conditions), the signal at 2.3 ppm shifts upfield to –3.0 ppm, which is consistent with an anionic, tetracoordinate boron species.[27] Thus, we assign the signal at –3.0 ppm as the ammonium O-boron enolate **1a-NH**.

Independent kinetic isotope effect (KIE) measurements were carried out using initial rates kinetics to probe the nature of the rate-determining step. A relatively large primary KIE of $k_H/k_D = 4.5 \pm 0.2$ was measured for the reaction of **1a** *vs* **1a-d$_8$** in toluene-d_8(Scheme 5a), consistent with the rate-determining transition state involving X-H bond cleavage. Additionally, the kinetic order of each reactant and catalyst was experimentally determined via reaction progress kinetic analysis (RPKA)[28] (See Supporting Information for details) using ketone **1a** and 1,3-enyne **2a** as model substrates. Different-excess experiments revealed a zero-order dependence of the reaction rate on both substrates (**1a** and **2a**), and a first order dependence on the total palladium catalyst concentration $[Pd/L]_0$. The reaction orders with respect to the total concentrations of Lewis acid catalyst $[B(C_6F_5)_3]_0$, and amine base catalyst $[PMP]_0$ depend on their relative catalyst loadings. When the Lewis acid is in excess of the base, the reaction is inverse first order in $[B(C_6F_5)_3]_0$, and first order in $[PMP]_0$. When the base is in excess of the Lewis acid, the reaction is zero order in $[B(C_6F_5)_3]_0$ and zero order in $[PMP]_0$ (Scheme 5b).

Scheme 5. Kinetic Isotope Effect, Rate Law, and Proposed Mechanism

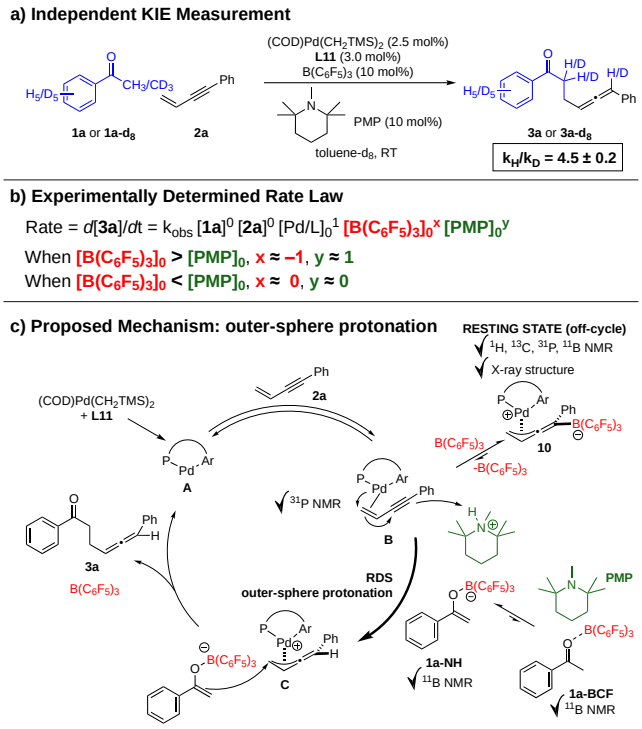

A proposed catalytic cycle is illustrated in Scheme 5c. In the presence of **L11**, the palladium precursor undergoes reductive elimination and loss of its COD ligand to form Pd(0)/Senphos complex **A**, which binds enyne **2a** to form **B**. Intermediate **B** exists in equilibrium with the off-cycle complex **10** which we have identified as the resting state of the Pd catalyst. For productive catalysis to occur, **10** must dissociate $B(C_6F_5)_3$ to reform **B**, which undergoes a rate-determining outer-sphere protonation[7a,29,30] of the palladium-bound enyne with ammonium enolate **1a-NH** to generate **C**. Intermediate **C** is then attacked by the boron enolate to generate the product **3a** and regenerate the palladium catalyst **A** and the $B(C_6F_5)_3$ catalyst.

This cooperative catalytic system can be broken down into two catalytic cycles: 1) Pd-based cycle acting on the enyne substrate (**2a**), and 2) $B(C_6F_5)_3$/PMP-based "cycle" acting on the ketone substrate (**1a**). Each catalyst is saturated with its respective substrate (i.e., Pd catalyst is completely saturated with the 1,3-enyne substrate and the $B(C_6F_5)_3$/PMP catalysts are saturated with the ketone substrate to a large extent, see Schemes 3-4) in both

the resting state and the rate-limiting transition state, consistent with the observed zero-order kinetics with respect to both ketone (**1a**) and enyne (**2a**) substrates. The rate-determining step involves a proton transfer which is consistent with the observed primary kinetic isotope effect. When excess $B(C_6F_5)_3$ is present relative to the Pd/Senphos catalyst (standard conditions), the catalysis is inhibited due to formation of the catalytically inactive **10**, leading to inverse-first order contribution of $B(C_6F_5)_3$ to the rate-expression for product formation for the Pd-based cycle. A simplified approximated product-forming rate expression based on limiting parameters (e.g., equilibria from experimental data) is:

$$d[\mathbf{3a}]/dt \sim k_{obs}\,[\mathbf{2a}]^0\,[Pd/L]_0^{\,1}\,[B(C_6F_5)_3]_0^{\,-1}\,[\mathbf{1a\text{-}NH}]^1 \qquad (1)$$

The second $B(C_6F_5)_3$/PMP cycle contributes to the [**1a-NH**]^1 term of the "main" rate expression (eq (1)). In this $B(C_6F_5)_3$/PMP cycle, when one catalyst is in excess of the other, the catalyst in excess will also experience "saturation" with respect to the limiting catalyst and no longer "contributes" (i.e., zero-order kinetics) to the formation of the ammonium enolate [**1a-NH]**.[31] Thus, when $[B(C_6F_5)_3]_0 > [PMP]_0$, it follows that [**1a-NH] ~** $[PMP]_0^{\,1}$ [**1a**]^0, resulting in the overall expression:

$$d[\mathbf{3a}]/dt \sim k_{obs}\,[\mathbf{1a}]^0\,[\mathbf{2a}]^0\,[Pd/L]_0^{\,1}\,[B(C_6F_5)_3]_0^{\,-1}\,[PMP]_0^{\,1} \qquad (2)$$

On the other hand, when $[B(C_6F_5)_3]_0 < [PMP]_0$, it follows that [**1a-NH] ~** $[B(C_6F_5)_3]_0^{\,1}$ [**1a**]^0, resulting in the overall expression:

$$d[\mathbf{3a}]/dt \sim k_{obs}\,[\mathbf{1a}]^0\,[\mathbf{2a}]^0\,[Pd/L]_0^{\,1}\,[B(C_6F_5)_3]_0^{\,0}\,[PMP]_0^{\,0} \qquad (3)$$

The above simplified kinetic model (eqs (1)-(3)) is consistent with our observed co-catalyst concentration dependent rate laws as shown in Scheme 5b. Thus, our proposed mechanism, including the assignment of the resting states and rate-determining step, is consistent with all the experimentally observed spectroscopic and kinetic data.

Density Functional Theory (DFT) calculations were carried out at SMD[32](Toluene)-ωB97X-D[33]/SDD+f(Pd)[34], 6-31+G**(other atoms)//SMD(Toluene)-ωB97X-D/SDD

+f(Pd),6-31G**(other atoms) level of theory (see Supporting Information for computational details) to additionally probe the mechanism of the Pd(0)Senphos/$B(C_6F_5)_3$/PMP-catalyzed hydroalkylation of enynes. We computationally considered three mechanistic scenarios (See Supporting Information, Scheme S1): (1) Outer-sphere protonation pathway (i.e., mechanism illustrated in Scheme 5c), (2) Protodeboronation pathway where the resting state species **10** is protonated with PMP-H^+ with concomitant release of $B(C_6F_5)_3$ to form **C**,[35] (3) Pd(II)–H pathway where the PMP-H^+ oxidatively adds to Pd(0) species **A** to form a Pd(II)-H intermediate that then subsequently undergoes β-migratory insertion[14b,36] into the 1,3-enyne to furnish the *syn*-diastereomer of the π-allyl intermediate **C** (i.e., H and Pd are oriented *syn* to each other).

DFT calculations predict that the Pd(0)/Senphos complex **A** coordinates to the C=C double bond of the 1,3-enyne to form the π-complex **B** in an exergonic fashion (Figure 1). We considered two possible isomers for the π-complex (See Supporting Information, Figures S1 and S2): **B** (alkene is *cis* to the P atom of the Senphos ligand) and **B'** (alkene is *trans* to the P atom of the Senphos ligand). Structure **B** has been found to be more stable (by > 1.3 kcal/mol) than **B'** throughout the reaction coordinate. This predicted orientational preference is consistent with the obtained crystal structure for the resting state complex **10** (Scheme 3c). The π-complex **B** kinetically prefers ($\Delta G^{\ddagger}_{B\text{-}10}$ = 9.6 kcal/mol) to undergo an outer-sphere oxidative addition with $B(C_6F_5)_3$ to furnish complex **10** via an early transition state $\mathbf{TS_{B\text{-}10}}$ (B…C_α: 2.493 Å and $\Sigma B_{\angle}$: 352.45°). Intermediate **10** is the computationally predicted resting state of the Pd catalyst, which agrees with the experimentally observed data (spectroscopic evidence, see Scheme 3; kinetic evidence, see Scheme 5b). The optimized structure of the Pd-π-allyl intermediate **10** (Pd–C_β, Pd–C_γ, Pd–C_δ: 2.346, 2.182 and 2.088 Å, respectively; B–C_α: 1.702 Å) reproduces the obtained X-ray crystallographic data.

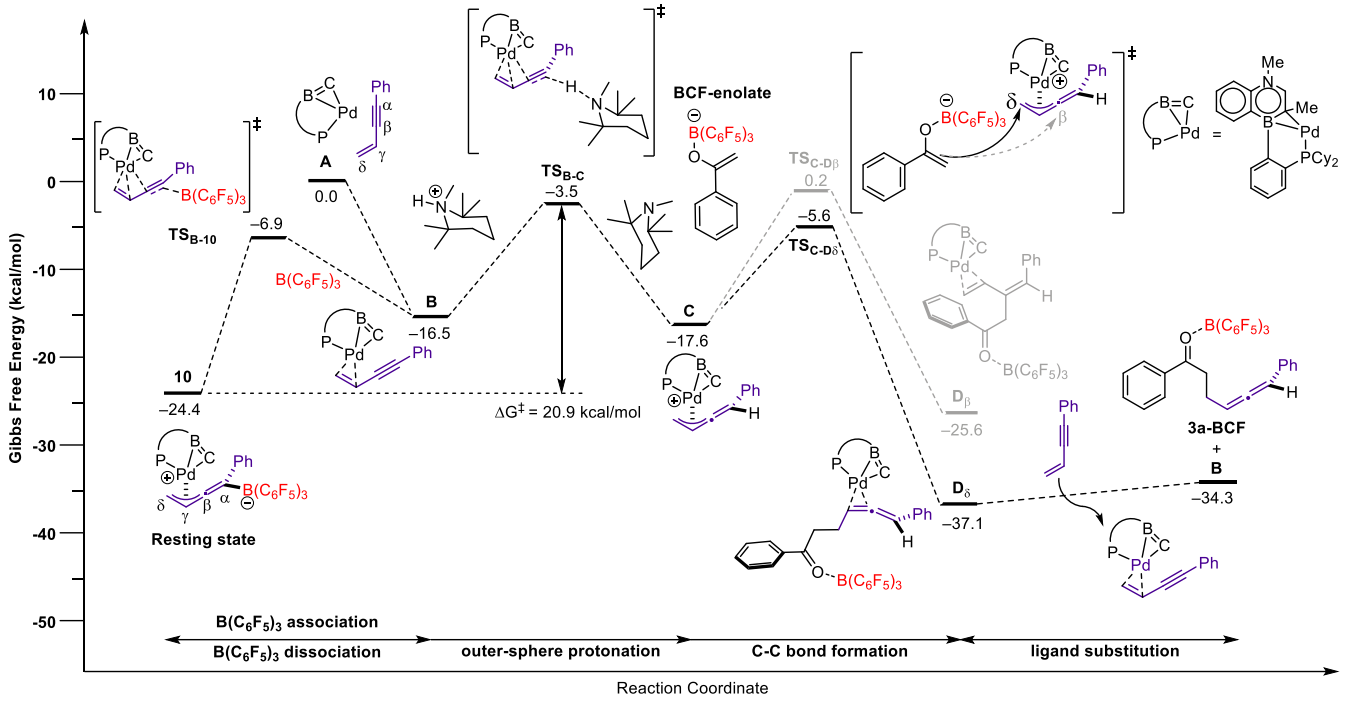

Figure 1. Energy profile (ΔG in kcal/mol) computed at SMD(Toluene)- ωB97X-D/SDD+f(Pd), 6-31G+**(other atoms)// SMD(Toluene)- ωB97X-D/SDD+f(Pd), 6-31G**(other atoms) level of theory for the proposed outer-sphere protonation mechanism where the protonated amine base PMP-H$^+$ oxidatively activates the Pd-enyne complex **B**. For the energy profiles of alternative mechanisms, see Supporting Information.

Complex **10** can readily dissociate $B(C_6F_5)_3$ to reform π-complex **B** ($\Delta G^{‡}_{10\rightarrow TSB\text{-}10}$ = 17.5 kcal/mol), which can then be protonated by PMP-H$^+$ (i.e., the proton source component of the ion pair **1a-NH**, N–H: 1.025 Å) with a barrier $\Delta G^{‡}_{B\text{-}C}$ = 13.0 kcal/mol to form the alkylidene-π-allylpalladium intermediate **C** ($C_α$–H: 1.091 Å; Pd–$C_β$, Pd–$C_γ$, Pd–$C_δ$: 2.144, 2.154 and 2.166 Å, respectively). In the transition state **TS$_{B\text{-}C}$**, the $C_α$…H and N…H bonds are 1.425 and 1.292 Å, respectively, and the ∠$C_α$HN = 175° bond angle is almost linear. In contrast to the structure of intermediate **C**, the allyl moiety in **TS$_{B\text{-}C}$** is non-symmetrically coordinated to Pd (Pd–$C_β$, Pd–$C_γ$, Pd–$C_δ$: 2.527, 2.201 and 2.076 Å, respectively), which is consistent with the Pd mostly maintaining an η^2 coordination with the alkene. From **C**, a nucleophilic attack by the **BCF-enolate** (i.e., the boron enolate component of the ion pair **1a-NH)** occurs with a $\Delta\Delta G^{‡}$ = 5.8 kcal/mol kinetic preference toward the $C_δ$ position over the $C_β$ position to generate the allene product **D$_δ$**. Product **3a** is then released

to start a new catalytic cycle. The nucleophilic attack is relatively facile with a predicted barrier of $\Delta G^{\ddagger}_{\mathbf{C\rightarrow TSC\text{-}D\delta}}$ = 12.0 kcal/mol. The calculated overall rate-limiting barrier $\Delta G^{\ddagger}_{\mathbf{10\rightarrow TSB\text{-}C}}$ of 20.9 kcal/mol, the predicted k_H/k_D(DFT) = 6.1, and the off-cycle resting state **10** for the proposed outer-sphere protonation pathway are consistent with experimental observations.

For mechanistic scenario (2): the protodeboronation pathway (see Supporting Information, Figure S3), DFT calculations show that the protodeboronation process occurs in 2 steps: i) a proton transfer from PMP-H^+ to C_β carbon of complex **10**, which is followed by ii) a [1,2]-H(hydride) shift from C_β to C_α position with concomitant release of $B(C_6F_5)_3$ to furnish **C**. The predicted rate-limiting barrier for this pathway is $\Delta G^{\ddagger}$= 48.1 kcal/mol, which is inconsistent with a room-temperature reaction.

For mechanistic scenario (3): the Pd(II)–H pathway (see Supporting Information, Figure S4), we computed the energy profile involving direct protonation of Pd(0)/Senphos complex **A** by PMP-H^+ followed by Pd-H β-migratory insertion into the triple bond of the 1,3-enyne. The direct protonation of Pd complex **A** is predicted to be energetically costly, with a rate-limiting barrier of $\Delta G^{\ddagger}$= 52.7 kcal/mol (from the resting state **10**), which is also inconsistent with a room-temperature reaction.

Conclusions

We have developed a mild, general method for hydroalkylation of 1,3-enynes with ketones to generate allenes. A broad range of aryl and alkyl ketones could be coupled with 1,3-enynes to provide synthetically useful β-allenyl ketones in high yield. To our knowledge, this work represents a rare example of room-temperature metal-catalyzed addition of a ketone α-C-H bond to an unsaturated hydrocarbon. Mechanistic studies reveal that the outer-sphere oxidative addition adduct **10** is an off-cycle resting state during catalysis. The rate-determining step involves a proton transfer with an accessible activation barrier computed at 20.9 kcal/mol. DFT calculations are in agreement with experimental kinetics and spectroscopic observations. The body of our mechanistic investigations points

toward a multifaceted and intricate behavior underlying the Pd/Senphos-catalyzed activation of 1,3-enynes, and we hope this work will serve as inspiration for the further development of mild and general catalytic systems which activate C(sp_3)-H bonds for addition to C-C π-bonds.

ASSOCIATED CONTENT

The Supporting Information is available free of charge at https://pubs.acs.org. Experimental procedures, compound characterization data, computational and crystallographic information (PDF)
Optimized Cartesian coordinates (XYZ)

Accession Codes

CCDC 2278579 and 2278580 contain the supplementary crystallographic data for this paper. These data can be obtained free of charge via www.ccdc.cam.ac.uk/data_request/cif, or by emailing data_request@ccdc.cam.ac.uk, or by contacting The Cambridge Crystallographic Data Centre, 12 Union Road, Cambridge CB2 1EZ, UK; fax: +44 1223 336033.

AUTHOR INFORMATION

Corresponding Author

Shih-Yuan Liu − Department of Chemistry, Boston College, Chestnut Hill, Massachusetts 02467-3860, United States, and Université de Pau et des Pays de l'Adour, E2S UPPA, Institut des Sciences Analytiques et de Physico-Chimie pour l'Environnement et les Matériaux IPREM UMR 5254. Hélioparc, 2 avenue P. Angot, 64053 Pau cedex 09, France; orcid.org/0000-0003-3148-9147; Email: shihyuan.liu@bc.edu

Karinne Miqueu – Université de Pau et des Pays de l'Adour, E2S UPPA / CNRS, Institut des Sciences Analytiques et de Physico-Chimie pour l'Environnement et les Matériaux IPREM UMR 5254. Hélioparc, 2 avenue P. Angot, 64053 Pau cedex 09, France; orcid.org/0000-0002-5960-1877; Email : karinne.miqueu@univ-pau.fr

Authors

Maxwell Eaton – Department of Chemistry, Boston College, Chestnut Hill, Massachusetts 02467-3860, United States

Yuping Dai – Université de Pau et des Pays de l'Adour, E2S UPPA / CNRS, Institut des Sciences Analytiques et de Physico-Chimie pour l'Environnement et les Matériaux IPREM UMR 5254. Hélioparc, 2 avenue P. Angot, 64053 Pau cedex 09, France

Ziyong Wang – Department of Chemistry, Boston College, Chestnut Hill, Massachusetts 02467-3860, United States

Bo Li – Department of Chemistry, Boston College, Chestnut Hill, Massachusetts 02467-3860, United States

Walid Lamine – Université de Pau et des Pays de l'Adour, E2S UPPA / CNRS, Institut des Sciences Analytiques et de Physico-Chimie pour l'Environnement et les Matériaux IPREM UMR 5254. Hélioparc, 2 avenue P. Angot, 64053 Pau cedex 09, France

Author Contributions

M. E. performed the experimental synthetic and mechanistic work guided by S.-Y. L. Y. D. performed the computational work guided by K. M. Z. W. discovered the title reaction and performed preliminary reaction optimization. B. L. solved the X-ray structures. W. L. provided initial computational analysis. The manuscript was written through contributions of all authors. All authors have given approval to the final version of the manuscript.

Notes

The authors declare no competing financial interests.

ACKNOWLEDGMENT

This work is dedicated to Prof. Gregory C. Fu on the occasion of his 60th birthday. Research reported in this publication was supported by the National Institute of General Medical Sciences of the National Institutes of Health (NIGMS) under Award Number R01GM136920, the Excellence Initiative of Université de Pau et des Pays de l'Adour I-Site E2S UPPA, and by Boston College start-up funds. We also acknowledge the NIH-S10 (award: 1S10OD026910-01A1) and the NSF-MRI (award: CHE-2117246) for the support of Boston College's NMR facilities. Part of this work was granted access to the HPC resources of [CCRT/CINES/IDRIS] under the allocation 2022 [AD010800045R1] made by GENCI (Grand Equipement National de Calcul Intensif) and Mésocentre de Calcul Intensif Aquitain (MCIA). The "Direction du Numérique" of UPPA is also acknowledged for supporting computational facilities. Z.W. was supported as a LaMattina Graduate Fellow in Chemical Synthesis. Y. D. and W. L were funded as a Ph.D. and postdoctoral fellow, respectively, by I-Site E2S-UPPA.

REFERENCES

(1) For an overview, see: (a) Hoffmann-Röder, A.; Krause, N. Synthesis and Properties of Allenic Natural Products and Pharmaceuticals. *Angew. Chem., Int. Ed.* **2004**, *43*, 1196-1216. (b) Rivera-Fuentes, P.; Diederich, F. Allenes in Molecular Materials. *Angew. Chem., Int. Ed.* **2012**, *51*, 2818-2828.

(2) Ma, S. Some Typical Advances in the Synthetic Applications of Allenes. *Chem. Rev.* **2005**, *105*, 2829-2872.

(3) Allen, A. D.; Tidwell, T. T. Ketenes and Other Cumulenes as Reactive Intermediates. *Chem. Rev.* **2013**, *113*, 7287-7342.

(4) Yu, S.; Ma, S. Allenes in Catalytic Asymmetric Synthesis and Natural Product Syntheses. *Angew. Chem., Int. Ed.* **2012**, *51*, 3074-3112.

(5) For an overview, see: (a) Yu, S.; Ma, S. How easy are the syntheses of allenes? *Chem. Commun*. **2011**, *47*, 5384-5418. (b) Neff, R. K.; Frantz, D. E. Recent advances in the catalytic syntheses of allenes: a critical assessment. *ACS Catal.* **2014**, *4*, 519-528.

(6) For hydrofunctionalization of enynes, see: (a) Yamamoto, Y.; Radhakrishnan, U. Palladium catalysed pronucleophile addition to unactivated carbon–carbon multiple bonds. *Chem. Soc. Rev.* **1999**, *28*, 199-207. (b) Salter, M. M.; Gevorgyan, V.; Saito, S.; Yamamoto, Y. Synthesis of Allenes via Palladium Catalysed Addition of Certain Activated Methynes to Conjugated Enynes. *Chem. Commun*. **1996**, *32*, 17-18. (c) Radhakrishnan, U.; Al-Masum, M.; Yamamoto, Y. Palladium Catalyzed Hydroamination of Conjugated Enynes. *Tetrahedron Lett.* **1998**, *39*, 1037-1040. (d) Fu, L.; Greßies, S.; Chen, P.; Liu, G. Recent Advances and Perspectives in Transition Metal-Catalyzed 1,4-Functionalizations of Unactivated 1,3-Enynes for the Synthesis of Allenes. *Chin. J. Chem*. **2020**, *38*, 91-100. (e) Dherbassy, Q.; Manna, S.; Talbot, F. J. T.; Prasitwatcharakorn, W.; Perry, G. J. P.; Procter, D. Copper-catalyzed functionalization of enynes. *Chem. Sci.* **2020**, *11*, 11380-11393. (f) Adamson, N. J.; Jeddi, H.; Malcolmson, S. J. Preparation of Chiral Allenes through Pd-Catalyzed Intermolecular Hydroamination of Conjugated Enynes: Enantioselective Synthesis Enabled by Catalyst Design. *J. Am. Chem. Soc.* **2019**, *141*, 8574–8583.

(7) For enantioselective hydroalkylation of 1,3-enynes to prepare allenes, see: (a) Tsukamoto, H.; Konno, T.; Ito, K.; Doi, T. Palladium(0)-Lithium Iodide Cocatalyzed Asymmetric Hydroalkylation of Conjugated Enynes with Pronucleophiles Leading to 1,3-Disubstituted Allenes. *Org. Lett.* **2019**, *21*, 6811-6814. (b) Yang, S.-Q.; Wang, Y.-F.; Zhao, W.-C.; Lin, G.-Q.; He, Z.-T. Stereodivergent Synthesis of Tertiary Fluoride-Tethered Allenes via Copper and Palladium Dual Catalysis. *J. Am. Chem. Soc*. **2021,** *143*, 7285-7291. (c) Qian, H.; Yu, X.; Zhang, J.; Sun, J. Organocatalytic enantioselective synthesis of 2,3-allenoates by intermolecular addition of nitroalkanes to activated enynes. *J. Am. Chem. Soc.* **2013**, *135*, 18020-18023. (d) Yao, Q.; Liao, Y.; Lin, L.; Lin, X.; Ji, J.; Liu, X.; Feng, X. Efficient Synthesis of Chiral Trisubstituted 1,2-Allenyl Ketones by Catalytic Asymmetric Conjugate Addition of Malonic Esters to Enynes. *Angew. Chem., Int. Ed*. **2016**, *55*, 1859-1863.

(8) For *intramolecular* hydroalkylation of olefins with ketones, see: (a) Wang, X.; Pei, T.; Han, X.; Widenhoefer, R. A. Palladium-catalyzed intramolecular hydroalkylation of unactivated olefins with dialkyl ketones. *Org. Lett.* **2003**, *5*, 2699–2701. (b) Xiao, Y.-P.; Liu, X.-Y.; Che, C.-M. Efficient gold(I)-catalyzed direct intramolecular hydroalkylation of unactivated alkenes with α-ketones. *Angew. Chem., Int. Ed.* **2011**, *50*, 4937–4941.

(9) For hydroalkylation of *styrene derivatives* with ketones, see: (a) Rodriguez, A. L.; Bunlaksananusorn, T.; Knochel, P. Potassium *tert*-butoxide catalyzed addition of carbonyl derivatives to styrenes. *Org. Lett.* **2000**, *2*, 3285-3287. (b) Majima, S.; Shimizu, Y.; Kanai, M. Cu(I)-catalyzed α-alkylation of ketones with styrene derivatives. *Tetrahedron Lett.* **2012**, *53*, 4381-4384. (c) Qiao, J.; Ci, R. N.; Gan, Q. C.; Huang, C.; Liu, Z.; Hu, H. L.; Ye, C.; Chen, B.; Tung, C. H.; Wu, L. Z. Amine-Free, Directing-Group-Free and Redox-Neutral alpha-Alkylation of Saturated Cyclic Ketones. *Angew. Chem., Int. Ed.* **2023**, *62*, e202305679.

(10) For hydroalkylation reactions with *aldehydes* via SOMO activation, see: (a) Comito, R. J.; Finelli, F. G.; MacMillan, D. W. C. Enantioselective intramolecular aldehyde α-alkylation with simple olefins: Direct access to homo-ene products. *J. Am. Chem. Soc*. **2013**, *135*, 9358-9361. (b) Beeson, T. D.; Mastracchio, A.; Hong, J. B.; Ashton, K.; Macmillan, D. W. C. Enantioselective organocatalysis using SOMO activation. *Science* **2007**, *316*, 582-585.

(11) (a) Mo, F.; Dong, G. Regioselective ketone α-alkylation with simple olefins via dual activation. *Science* **2014**, *345*, 68-72. (b) Xing, D.; Dong, G. Branched-Selective Intermolecular Ketone α-Alkylation with Unactivated Alkenes via an Enamide Directing Strategy. *J. Am. Chem. Soc.* **2017**, *139*, 13664-13667.

(12) Cheng, L.; Li, M.-M.; Xiao, L.-J.; Xie, J.-H.; Zhou, Q.-L. Nickel(0)-Catalyzed Hydroalkylation of 1,3-Dienes with Simple Ketones *J. Am. Chem. Soc.* **2018**, *140* , 11627-11630.

(13) For amine/transition metal-cocatalyzed hydroalkylation using ketones and aldehydes, see: (a) Yang, C.; Zhang, K.; Wu, Z.; Yao, H.; Lin, A. Cooperative Palladium/Proline-Catalyzed Direct α-Allylic Alkylation of Ketones with Alkynes *Org. Lett.* **2016**, *18*, 5332-5335. (b) Zhou, H.; Wang, Y.; Zhang, L.; Cai, M.; Luo, S. Enantioselective Terminal Addition to Allenes by Dual Chiral Primary Amine/Palladium Catalysis. *J. Am. Chem. Soc.*

2017, *139*, 3631–3634. (c) Cruz, F. A.; Dong, V. M. Stereodivergent Coupling of Aldehydes and Alkynes via Synergistic Catalysis Using Rh and Jacobsen's Amine. *J. Am. Chem. Soc.* **2017**, *139*, 1029–1032.

(14) For intermolecular hydroalkylation of dienes and other unsaturated hydrocarbons with activated pronucleophiles, see: (a) Adamson, N. J.; Wilbur, K. C. E.; Malcolmson, S. J. Enantioselective Intermolecular Pd-Catalyzed Hydroalkylation of Acyclic 1,3-Dienes with Activated Pronucleophiles. *J. Am. Chem. Soc.* **2018**, *140*, 2761-2764. (b) Park, S.; Adamson, N. J.; Malcolmson, S. J. Bronsted acid and Pd-PHOX dual-catalysed enantioselective addition of activated C-pronucleophiles to internal dienes. *Chem. Sci.* **2019**, *10*, 5176-5182. (c) Adamson, N. J.; Park, S.; Zhou, P.; Nguyen, A. L.; Malcolmson, S. J. Enantioselective Construction of Quaternary Stereogenic Centers by the Addition of an Acyl Anion Equivalent to 1,3-Dienes. *Org. Lett.* **2020**, *22*, 2032-2037. (d) Leitner, A.; Larsen, J.; Steffens, C.; Hartwig, J. F. Palladium-Catalyzed Addition of Mono- and Dicarbonyl Compounds to Conjugated Dienes. *J. Org. Chem.* **2004**, *69*, 7552–7557. (e) Trost, B. M.; Simas, A. B. C.; Plietker, B.; Jäkel, C.; Xie, J. Enantioselective Palladium-Catalyzed Addition of 1,3-Dicarbonyl Compounds to an Allene Derivative. *Chem. Eur. J.* **2005**, *11*, 7075–7082. (f) Zhang, Q.; Yu, H.; Shen, L.; Tang, T.; Dong, D.; Chai, W.; Zi, W. Stereodivergent Coupling of 1,3-Dienes with Aldimine Esters Enabled by Synergistic Pd and Cu Catalysis. *J. Am. Chem. Soc.* **2019**, *141*, 14554–14559. (g) Shao, W.; Besnard, C.; Guénée, L.; Mazet, C. Ni-Catalyzed Regiodivergent and Stereoselective Hydroalkylation of Acyclic Branched Dienes with Unstabilized C(Sp3) Nucleophiles. *J. Am. Chem. Soc.* **2020**, *142*, 16486–16492. (h) Yang, H.; Xing, D. Palladium-Catalyzed Diastereo- and Enantioselective Allylic Alkylation of Oxazolones with 1,3-Dienes under Base-Free Conditions. *Chem. Commun.* **2020**, *56*, 3721–3724. (i) Zhang, Z.; Xiao, F.; Wu, H.-M.; Dong, X.-Q.; Wang, C.-J. Pd-Catalyzed Asymmetric Hydroalkylation of 1,3-Dienes: Access to Unnatural α-Amino Acid Derivatives Containing Vicinal Quaternary and Tertiary Stereogenic Centers. *Org. Lett.* **2020**, *22*, 569–574. (j) Wang, H.; Zhang, R.; Zhang, Q.; Zi, W. Synergistic Pd/Amine-Catalyzed Stereodivergent Hydroalkylation of 1,3-Dienes with Aldehydes: Reaction Development, Mechanism, and Stereochemical Origins. *J. Am. Chem. Soc.* **2021**, *143*, 10948–10962. (k) Chen, X.-X.; Luo, H.; Chen, Y.-W.; Liu, Y.; He, Z.-T. Enantioselective Palladium-Catalyzed Directed Migratory Allylation of Remote Dienes. *Angew. Chem. Int. Ed.* **2023**, *62*, e202307628. (l) Wang, X.; Miao, H.-Z.; Lin, G.-Q.; He, Z.-T. Ligand-Dictated Regiodivergent Allylic Functionalizations via Palladium-Catalyzed Remote Substitution. *Angew. Chem. Int. Ed.* **2023**, *62*, e202301556.

(15) For addition of beta-ketoacids to alkynes, see: (a) Cruz, F. A.; Chen, Z.; Kurtoic, S. I.; Dong, V. M. Tandem Rh-Catalysis: Decarboxylative β-Keto Acid and Alkyne Cross-Coupling. *Chem. Commun.* **2016**, *52*, 5836–5839. (b) Li, C.; Grugel, C. P.; Breit, B. Rhodium-Catalyzed Chemo- and Regioselective Decarboxylative Addition of β-Ketoacids to Alkynes. *Chem. Commun.* **2016**, *52*, 5840–5843.

(16) Foley, D. J.; Waldmann, H. Ketones as strategic building blocks for the synthesis of natural product-inspired compounds. *Chem. Soc. Rev*. **2022**, *51*, 4094-4120.

(17) (a) Xu, S.; Zhang, Y.; Li, B.; Liu, S.-Y. Site- and Stereo-selective *trans*-Hydroboration of 1,3-Enynes Catalyzed by 1,4-Azaborine-Based Phosphine-Pd Complex. *J. Am. Chem. Soc.* **2016**, *138*, 14566-14569. (b) Zhang, Y.; Li, B.; Liu, S.-Y. Pd-Senphos Catalyzed *trans*-Selective Cyanoboration of 1,3-Enynes. *Angew. Chem., Int. Ed*. **2020**, *59*, 15928-15932. (c) Wang, Z.; Wu, J.; Lamine, W.; Li, B.; Sotiropoulos, J.-M.; Chrostowska, A.; Miqueu, K.; Liu, S.-Y. C-Boron Enolates Enable Palladium Catalyzed Carboboration of Internal 1,3-Enynes. *Angew. Chem., Int. Ed.* **2021**, *60*, 21231-21236.

(18) (a) Yang, Y.; Jiang, J.; Yu, H.; Shi, J. Mechanism and Origin of the Stereoselectivity in the Palladium-Catalyzed *trans* Hydroboration of Internal 1,3-Enynes with an Azaborine-Based Phosphine Ligand. *Chem. Eur. J.* **2018**, *24*, 178-186. (b) Zhang, Y.; Wang, Z.; Lamine, W.; Xu, S.; Li, B.; Chrostowska, A.; Miqueu, K.; Liu, S.-Y., Mechanism of Pd/Senphos-Catalyzed *trans*-Hydroboration of 1,3-Enynes: Experimental and Computational Evidence in Support of the Unusual Outer-Sphere Oxidative Addition Pathway. *J. Org. Chem.* **2023**, *88*, 2415-2424. (c) Wang, Z.; Lamine, W.; Miqueu, K.; Liu, S.-Y., A *syn* outer-sphere oxidative addition: the reaction mechanism in Pd/Senphos-catalyzed carboboration of 1,3-enynes. *Chem. Sci.* **2023**, *14*, 2082-2090.

(19) Wang, Z.; Zhang, C.; Wu, J.; Li, B.; Chrostowska, A.; Karamanis, P.; Liu, S.-Y., *trans*-Hydroalkynylation of Internal 1,3-Enynes Enabled by Cooperative Catalysis. *J. Am. Chem. Soc.* **2023**, *145*, 5624-5630.

(20) For cooperative activation of ketones by $B(C_6F_5)_3/NR_3$, see: (a) Chan, J. Z.; Yao, W.; Hastings, B. T.; Lok, C. K.; Wasa, M. Direct Mannich-Type Reactions Promoted by Frustrated Lewis Acid/Brønsted Base Catalysts. *Angew. Chem., Int. Ed.* **2016**, *55*, 13877-13881. (b) Shang, M.; Wang, X.; Koo, S. M.; Youn, J.; Chan, J. Z.; Yao, W.; Hastings, B. T.; Wasa, M. Frustrated Lewis Acid/Brønsted Base Catalysts for Direct Enantioselective α-Amination of Carbonyl Compounds. *J. Am. Chem. Soc.* **2017**, *139*, 95-98. (c) Lam, J.; Szkop, K. M.; Mosaferi, E.; Stephan, D. W. FLP catalysis: main group hydrogenations of organic unsaturated substrates. *Chem. Soc. Rev.* **2019**, *48*, 3592-3612.

(21) Xu, S.; Haeffner, F.; Li, B.; Zakharov, L. N.; Liu, S.-Y. Monobenzofused 1,4-azaborines: synthesis, characterization, and discovery of a unique coordination mode. *Angew. Chem., Int. Ed.* **2014**, *53*, 6795-6799.

(22) Reetz, M. T.; Kyung, S. H.; Hüllmann, M. CH3Li/TiCl4: A Non-Basic and Highly Selective Grignard Analogue. *Tetrahedron* **1986**, *42*, 2931–2935.

(23) Zhang, Z.; Liu, C.; Kinder, R. E.; Han, X.; Qian, H.; Widenhoefer, R. A. Highly Active Au(I) Catalyst for the Intramolecular Exo-Hydrofunctionalization of Allenes with Carbon, Nitrogen, and Oxygen Nucleophiles. *J. Am. Chem. Soc.* **2006**, *128*, 9066–9073.

(24) Yang, Y.; Perry, I. B.; Lu, G.; Liu, P.; Buchwald, S. L. Copper-Catalyzed Asymmetric Addition of Olefin-Derived Nucleophiles to Ketones. *Science* **2016**, *353*, 144–150.

(25) Meng, F.; Jang, H.; Jung, B.; Hoveyda, A. H. Cu-Catalyzed Chemoselective Preparation of 2-(Pinacolato)Boron-Substituted Allylcopper Complexes and Their In Situ Site-, Diastereo-, and Enantioselective Additions to Aldehydes and Ketones. *Angew. Chem., Int. Ed.* **2013**, *52*, 5046–5051.

(26) Parks, D. J.; Piers, W. E.; Parvez, M.; Atencio, R.; Zaworotko, M. J. Synthesis and solution and solid-state structures of tris(pentafluorophenyl)borane adducts of PhC(O)X (X = H, Me, OEt, Ni-Pr_2). *Organometallics* **1998**, *17*, 1369-1377.

(27) Blackwell, J. M.; Piers, W. E.; McDonald, R. Mechanistic Studies on the $B(C_6F_5)_3$ Catalyzed Allylstannation of Aromatic Aldehydes with Ortho Donor Substituents. *J. Am. Chem. Soc.* **2002**, *124*, 1295-1306.

(28) Blackmond, D. G. Reaction Progress Kinetic Analysis: A Powerful Methodology for Mechanistic Studies of Complex Catalytic Reactions. *Angew. Chem., Int. Ed.* **2005**, *44*, 4302-4320.

(29) For stoichiometric protonation of unsaturated hydrocarbons coordinated to low-valent metals, see: (a) Casey, C. P.; Chung, S.; Ha, Y.; Powell, D. R. Formation of platinum allyl and propargyl complexes from protonation of platinum enyne and diyne complexes. *Inorg. Chim. Acta* **1997**, *265*, 127-138. (b) Casey, C. P.; Chung, S. Protonation of rhenium 1,3-enyne and 1,3-diyne complexes: formation of exo-alkylidene eta-3-allyl and eta-3-propargyl complexes. *Inorg. Chim. Acta* **2002**, *334*, 283-293.

(30) For catalytic examples of palladium-bound diyne protonation, see: (a) Camacho, D. H.; Saito, S.; Yamamoto, Y., 'Anti-Wacker'-type hydroalkoxylation of diynes catalyzed by palladium(0). *Tetrahedron Lett.* **2002**, *43*, 1085-1088. (b) Liu, J.; Schneider, C.; Yang, J.; Wei, Z.; Jiao, H.; Franke, R.; Jackstell, R.; Beller, M. A General and Highly Selective Palladium-Catalyzed Hydroamidation of 1,3-Diynes. *Angew. Chem., Int. Ed.* **2021**, *60*, 371- 379.

(31) Because the equilibrium favors the ammonium boron enolate species, the concentration of [**1a-NH**] can then be approximated as being equal to the concentration of the limiting catalyst.

(32) Marenich, A. V.; Cramer, C. J.; Truhlar, D. G. Universal Solvation Model Based on Solute Electron Density and on a Continuum Model of the Solvent Defined by the Bulk Dielectric Constant and Atomic Surface Tensions. *J. Phys. Chem. B.* **2009**, *113*, 6378-6396.

(33) Chai J.-D.; Head-Gordon M. Long-range Corrected Hybrid Density Functionals with Damped Atom–atom Dispersion Corrections. *Phys. Chem. Chem. Phys.* **2008**, *10*, 6615-6620.

(34) (a) Andrae, D.; Häussermann, U.; Dolg, M.; Stoll, H.; Preuss, H. Energy-adjusted ab-initio Pseudopotentials for the Second and Third Row Transition Elements. *Theor. Chim. Acta.* **1990**, *77*, 123-141. (b) Dolg, M. Modern Methods and Algorithm of Quantum Chemistry, Vol. 1. Grotendorst. J., John von Neuman Institute for Computing, Jülich (Germany), 2000, 479-501. (c) Ehlers, A.W.; Böhme, M.; Dapprich, S.; Gobbi, A.; Höllwarth, A.; Jonas, V.; Köhler, K. F.; Stegmann, R.; Veldkamp, A.; Frenking, G. A set of f-polarization Functions for Pseudo-potential Basis Sets of the Transition Metals Sc-Cu, Y-Ag and La-Au. *Chem. Phys. Lett.* **1993**, *208*, 111-114.

(35) Tamke, S.; Qu, Z. W.; Sitte, N. A.; Florke, U.; Grimme, S.; Paradies, J. Frustrated Lewis Pair-Catalyzed Cycloisomerization of 1,5-Enynes via a 5-endo-dig Cyclization/Protodeborylation Sequence. *Angew. Chem., Int. Ed.* **2016**, *55*, 4336−4339.

(36) Park, S.; Malcolmson, S. J. Development and Mechanistic Investigations of Enantioselective Pd-Catalyzed Intermolecular Hydroaminations of Internal Dienes. *ACS Catal.* **2018**, *8*, 8468-8476.